



Chronic PPAR γ Stimulation Shifts Amyloidosis to Higher Fibrillarity but Improves Cognition

OPEN ACCESS

Edited by:

Rodrigo Morales,
University of Texas Health Science
Center at Houston, United States

Reviewed by:

Jaqueline Generoso,
Universidade do Extremo Sul
Catarinense, Brazil
Raquel Sanchez-Varo,
Universidad de Málaga, Spain

*Correspondence:

Matthias Brendel
matthias.brendel@med.uni-
muenchen.de

† These authors have contributed
equally to this work

Specialty section:

This article was submitted to
Alzheimer's Disease and Related
Dementias,
a section of the journal
Frontiers in Aging Neuroscience

Received: 13 January 2022

Accepted: 25 February 2022

Published: 30 March 2022

Citation:

Blume T, Deussing M, Biechele G,
Peters F, Zott B, Schmidt C,
Franzmeier N, Wind K, Eckenweber F,
Sacher C, Shi Y, Ochs K,
Kleinberger G, Xiang X, Focke C,
Lindner S, Gildehaus F-J, Beyer L,
von Ungern-Sternberg B,
Bartenstein P, Baumann K,
Adelsberger H, Rominger A,
Cumming P, Willem M, Dorostkar MM,
Herms J and Brendel M (2022)
Chronic PPAR γ Stimulation Shifts
Amyloidosis to Higher Fibrillarity but
Improves Cognition.
Front. Aging Neurosci. 14:854031.
doi: 10.3389/fnagi.2022.854031

Tanja Blume^{1†}, Maximilian Deussing^{2†}, Gloria Biechele³, Finn Peters¹, Benedikt Zott^{4,5}, Claudio Schmidt², Nicolai Franzmeier⁶, Karin Wind^{1,2}, Florian Eckenweber², Christian Sacher², Yuan Shi¹, Katharina Ochs¹, Gernot Kleinberger^{7,8}, Xianyuan Xiang⁷, Carola Focke², Simon Lindner², Franz-Josef Gildehaus², Leonie Beyer², Barbara von Ungern-Sternberg², Peter Bartenstein², Karlheinz Baumann⁹, Helmuth Adelsberger³, Axel Rominger^{10,11}, Paul Cumming^{2,12}, Michael Willem⁷, Mario M. Dorostkar^{1,13}, Jochen Herms^{1,10,13†} and Matthias Brendel^{1,2,10*†}

¹ DZNE – German Center for Neurodegenerative Diseases, Munich, Germany, ² Department of Nuclear Medicine, University Hospital of Munich, Ludwig Maximilian University of Munich, Munich, Germany, ³ Department of Radiology, University Hospital of Munich, Ludwig Maximilian University of Munich, Munich, Germany, ⁴ Institute of Neuroscience, Technical University of Munich, Munich, Germany, ⁵ Department of Diagnostic and Interventional Neuroradiology, Klinikum Rechts der Isar, Technical University of Munich, Munich, Germany, ⁶ Institute for Stroke and Dementia Research, University Hospital of Munich, Ludwig Maximilian University of Munich, Munich, Germany, ⁷ Metabolic Biochemistry, Faculty of Medicine, Biomedical Center (BMC), Ludwig Maximilian University of Munich, Munich, Germany, ⁸ ISAR Bioscience GmbH, Planegg, Germany, ⁹ Roche Pharma Research and Early Development, Neuroscience Discovery, Roche Innovation Center Basel, F. Hoffmann-La Roche Ltd., Basel, Switzerland, ¹⁰ SyNergy, Ludwig Maximilian University of Munich, Munich, Germany, ¹¹ Department of Nuclear Medicine, Inselspital Bern, Bern, Switzerland, ¹² School of Psychology and Counselling, Queensland University of Technology, Brisbane, QLD, Australia, ¹³ Center for Neuropathology and Prion Research, Ludwig Maximilian University of Munich, Munich, Germany

We undertook longitudinal β -amyloid positron emission tomography (A β -PET) imaging as a translational tool for monitoring of chronic treatment with the peroxisome proliferator-activated receptor gamma (PPAR γ) agonist pioglitazone in A β model mice. We thus tested the hypothesis this treatment would rescue from increases of the A β -PET signal while promoting spatial learning and preservation of synaptic density. Here, we investigated longitudinally for 5 months PS2APP mice ($N = 23$; baseline age: 8 months) and App^{NL-G-F} mice ($N = 37$; baseline age: 5 months) using A β -PET. Groups of mice were treated with pioglitazone or vehicle during the follow-up interval. We tested spatial memory performance and confirmed terminal PET findings by immunohistochemical and biochemistry analyses. Surprisingly, A β -PET and immunohistochemistry revealed a shift toward higher fibrillary composition of A β -plaques during upon chronic pioglitazone treatment. Nonetheless, synaptic density and spatial learning were improved in transgenic mice with pioglitazone treatment, in association with the increased plaque fibrillarity. These translational data suggest that a shift toward higher plaque fibrillarity protects cognitive function and brain integrity. Increases in the A β -PET signal upon immunomodulatory treatments targeting A β aggregation can thus be protective.

Keywords: pioglitazone, A β -PET, App^{NL-G-F} mice, PS2APP mice, microglia, A β -plaque composition

INTRODUCTION

Alzheimer's disease (AD) has become the most common cause of dementia, and is imposing a significant burden on health care systems of societies with aging populations (Ziegler-Graham et al., 2008). During the past few decades, research on AD pathogenesis led to the formulation of a model that accumulation of amyloid beta (A β)-plaques and neurofibrillary tangles, the histologically characterizing hallmarks of AD (Braak and Braak, 1991), triggers a cascade of neurodegenerative events, leading to disease progression (Sasaguri et al., 2017). Additionally, novel emerging evidence indicates that neuroinflammation plays an important role in pathogenesis and progression of AD and many other neurodegenerative diseases (Zimmer et al., 2014; Heneka et al., 2015). In AD, activated microglial cells are able to bind and phagocytize soluble A β , and to some degree also the fibrillary A β aggregates, as part of the increased inflammatory response (Heneka et al., 2015). However, others report that A β -recognition receptors on microglia downregulate during the progression of AD, such that microglial cells eventually undergo senescence, characterized by reduced phagocytosis of A β -aggregates (Hickman et al., 2008). With time, the decreased microglial activity is permissive to expansion of fibrillar amyloidosis (Heppner et al., 2015; Blume et al., 2018) and a high proportion of dystrophic microglia were observed in human AD brain *post mortem* (Streit et al., 2014). These observations have led some to speculate that the microglial response is overwhelmed by the massive A β -deposition occurring in advanced AD, such that their chronic activation has a detrimental impact on disease progression (Hickman et al., 2008; Lee and Landreth, 2010).

It might follow that treatment with anti-inflammatory drugs should alleviate AD progression. Pioglitazone is an anti-inflammatory insulin sensitizer widely used to treat hyperglycemia in type 2 diabetes *via* activation of peroxisome proliferator-activated receptor gamma (PPAR- γ). Treatment with pioglitazone enables microglial cells to undergo a phenotypic conversion from a pro-inflammatory toward an anti-inflammatory and neuroprotective phenotype (Mandrekar-Colucci et al., 2012; Yamanaka et al., 2012). Furthermore, activation of PPAR- γ in the brains of AD mice initiate a coupled metabolic cycle with the Liver X Receptor to increase brain apolipoprotein E levels, which promotes the ability of microglial cells to phagocytose and degrade both soluble and fibrillary A β (Mandrekar-Colucci et al., 2012; Yamanaka et al., 2012). However, another study showed that only low-dose PPAR- γ agonist treatment, but not the conventional doses, promotes an A β -clearing effect by increasing (LDL Receptor Related Protein 1 (LRP1) in human brain microvascular endothelial cells (HBMECs) (Moon et al., 2012). Despite this compelling preclinical evidence, a meta-analysis encompassing nine clinical studies did not compelling support a beneficial effect of PPAR- γ agonist treatment on cognition and memory in in patients with mild-to-moderate AD (Cheng et al., 2016). Furthermore, a phase III trial of pioglitazone in patients with mild AD was discontinued due to lacking efficacy (Geldmacher et al., 2011). It remains a conundrum why the translation of PPAR- γ stimulation into human AD failed, which calls for

further investigation to uncover the basis of the seemingly false lead. Conceivably, the efficacy of pioglitazone may be confined to a specific stage of AD, or in cases distinguished by a particular biomarker.

Given this background, we hypothesized that A β -load and composition would determine the individual efficacy of PPAR- γ stimulation effect in the progression of AD mouse models. Therefore, we undertook serial small animal positron emission tomography (μ PET) with the A β -tracer [18 F]florbetaben (Manook et al., 2012; Rominger et al., 2013; Brendel et al., 2015a,b) in two AD mouse models with distinct A β -plaque composition. The transgenic PS2APP-line develops dense fibrillary A β -plaques with late debut whereas the knock-In mouse model *App*^{NL-G-F} develops more diffuse oligomeric A β -plaques with early debut. Both strains of mice were treated with pioglitazone or vehicle for 5 months during the phase of main A β accumulation. We conducted behavioral assessments of spatial learning and confirmed longitudinal PET findings by immunohistochemical analysis and biochemical analysis, thus aiming to test the hypothesis that response to pioglitazone would depend on the type of A β -plaques formed in transgenic mice.

MATERIALS AND METHODS

Study Design

Groups of PS2APP and *App*^{NL-G-F} mice were randomized to either treatment (PS2APP-PIO $N = 13$, all female; *App*^{NL-G-F}-PIO $N = 14$, $N = 10$ male, $N = 4$ female) or vehicle (PS2APP-VEH $N = 10$, all female; *App*^{NL-G-F}-VEH $N = 23$ $N = 9$ male, $N = 14$ female) groups at the age of 8 (PS2APP) and 5 (*App*^{NL-G-F}) months. In PS2APP mice, the baseline [18 F]florbetaben-PET scan (A β -PET) was performed at the age of 8 months, followed by initiation of pioglitazone treatment or vehicle for a period of 5 months and a follow-up A β -PET scan at 13 months. In *App*^{NL-G-F} mice, the baseline A β -PET scan was performed at the age of 5 month, followed by initiation of pioglitazone treatment or vehicle, for a period of 5 months. Follow-up A β -PET scans were acquired at 7.5 and 10 months of age, which was the study termination in *App*^{NL-G-F} mice. Mice were fed *ad libitum* with food pellets formulated with pioglitazone at a dose of 350 mg/kg or unaltered control pellets. The food was available to the mice without restriction.

For all mice, behavioral testing after the terminal PET scan was followed by immunohistochemical and biochemical analyses of randomized hemispheres. The TSPO-PET arm of the study and detailed analyses of neuroinflammation imaging are reported in a separate manuscript focusing on the predictive value of TSPO-PET for outcome of PPAR- γ -related immunomodulation (Biechele et al., 2022). The sample size estimation of the *in vivo* PET study was based on previous experience and calculated by G*power (V3.1.9.2, Kiel, Germany), assuming a type I error $\alpha = 0.05$ and a power of 0.8 for group comparisons, a 10% drop-out rate per time-point (including TSPO-PET), and a treatment effect of 5% change in the PET signal. Shared datapoints between the study arms are indicated.

Animals

PS2APP transgenic (Ozmen et al., 2008), *App*^{NL-G-F} APP knock-in (Saito et al., 2014) and wild-type C57Bl/6 mice were used in this investigation (for details see **Supplementary Material**). All experiments were performed in compliance with the National Guidelines for Animal Protection, Germany, with approval of the local animal care committee of the Government of Oberbayern (Regierung Oberbayern) and overseen by a veterinarian. The experiments complied with the ARRIVE guidelines and were carried out in accordance with the U.K. Animals (Scientific Procedures) Act, 1986 and associated guidelines, EU Directive 2010/63/EU for animal experiments. Animals were housed in a temperature and humidity-controlled environment with a 12-h light–dark cycle, with free access to food (Ssniff) and water.

A β -PET Acquisition and Reconstruction

[¹⁸F]florbetaben radiosynthesis was performed as previously described (Rominger et al., 2013). This procedure yielded a radiochemical purity exceeding 98% and a specific activity of 80 ± 20 GBq/ μ mol at the end of synthesis. Mice were anesthetized with isoflurane (1.5%, delivered *via* a mask at 3.5 L/min in oxygen) and received a bolus injection [¹⁸F]florbetaben 12 ± 2 MBq in 150 μ L of saline to a tail vein. Following placement in the tomograph (Siemens Inveon DPET), a single frame emission recording for the interval 30–60 min p.i., which was preceded by a 15-min transmission scan obtained using a rotating [⁵⁷Co] point source. The image reconstruction procedure consisted of three-dimensional ordered subset expectation maximization (OSEM) with four iterations and twelve subsets followed by a maximum *a posteriori* (MAP) algorithm with 32 iterations. Scatter and attenuation correction were performed and a decay correction for [¹⁸F] was applied. With a zoom factor of 1.0 and a $128 \times 128 \times 159$ matrix, a final voxel dimension of $0.78 \times 0.78 \times 0.80$ mm was obtained.

Small-Animal PET Data Analyses

Volumes of interest (VOIs) were defined on the MRI mouse atlas (Dorr et al., 2007). A forebrain target VOI (15 mm³) was used for group comparisons and an additional hippocampal target VOI (8 mm³) served for correlation analysis with spatial learning. We calculated [¹⁸F]florbetaben standard-uptake-value ratios (SUVRs) using the established white matter (PS2APP; 67 mm³; pons, midbrain, hindbrain and parts of the subcortical white matter) and periaqueductal gray (*App*^{NL-G-F}; 20 mm³) reference regions (Brendel et al., 2016; Overhoff et al., 2016; Sacher et al., 2019).

Water Maze

Two different water maze tasks were applied due to changing facilities between the investigations of PS2APP and *App*^{NL-G-F} cohorts. We used a principal component analysis of the common read outs of each water maze task to generate a robust index for correlation analyses in individual mice (Biechele et al., 2020). The principal component of the water maze test was extracted from three spatial learning read-outs (PS2APP: escape latency, distance, platform choice; *App*^{NL-G-F}: escape latency, frequency to platform, time spent

in platform quadrant). Thus, one quantitative index of water maze performance per mouse was generated for correlation with PET imaging readouts. The experimenter was blind to the phenotype of the animals.

Water Maze in PS2APP Mice

PS2APP and age-matched wild-type mice were subjected to a modified Morris water maze task as described previously (Sauvage et al., 2000; Busche et al., 2015; Keskin et al., 2017; Focke et al., 2019) yielding escape latency, distance to the correct platform and correct choice of the platform as read-outs.

Water Maze in *App*^{NL-G-F} Mice

App^{NL-G-F} mice (treated and vehicle) and 14 age- and sex-matched wild-type mice (vehicle) underwent a classical Morris water maze test, which was performed according to a standard protocol with small adjustments (Bromley-Brits et al., 2011) as previously described (Sacher et al., 2019). Details are provided in the **Supplementary Material**.

Immunohistochemistry

Immunohistochemistry in brain regions corresponding to PET analyses was performed for fibrillary as well as pre-fibrillary A β , microglia and synaptic density as previously published (Dorostkar et al., 2010; Brendel et al., 2017a,b). We obtained immunofluorescence labeling of pre-fibrillary A β using NAB228 (Thermo Fisher Scientific, Waltham, Massachusetts, United States) with a dilution of 1:500 (Monasor et al., 2020). For histological staining against fibrillar A β , we used methoxy-X04 (TOCRIS, Bristol, United Kingdom) at a dilution of 0.01 mg/ml in the same slice as for NAB228 staining. We obtained immunofluorescence labeling of microglia using an Iba-1 antibody (Wako, Richmond, United States) with a dilution of 1:200 co-stained with CD68 (BioRad, Hercules, CA, United States) with a dilution of 1:100. The synaptic density was measured using an anti-vesicular glutamate transporter 1 (VGLUT1) primary antibody (1:500, MerckMillipore, Billerica, Massachusetts, United States). Quantification was calculated as area-%. Details are provided in the **Supplementary Material**.

Biochemical Characterization of Brain Tissue

DEA (0.2% Diethylamine in 50 mM NaCl, pH 10) and RIPA lysates (20 mM Tris-HCl (pH 7.5), 150 mM NaCl, 1 mM Na₂EDTA, 1% NP-40, 1% sodium deoxycholate, 2.5 mM sodium pyrophosphate) were prepared from brain hemispheres. The later was centrifuged at 14,000 g (60 min at 4°C) and the remaining pellet was homogenized in 70% formic acid (FA fraction). The FA fraction was neutralized with 20×1 M Tris-HCl buffer at pH 9.5 and used further diluted for A β analysis. A β contained in FA fractions was quantified by a sandwich immunoassay using the Meso Scale A β Triplex plates and Discovery SECTOR Imager 2400 as described previously (Page et al., 2008). Samples were measured in triplicates.

Statistics

The principal component of the water maze test was extracted using SPSS 26 statistics (IBM Deutschland GmbH, Ehningen,

Germany). Prior to the PCA, the linear relationship of the data was tested by a correlation matrix and items with a correlation coefficient < 0.3 were discarded. The Kaiser-Meyer-Olkin (KMO) measure and Bartlett's test of sphericity were used to test for sampling adequacy and suitability for data reduction. Components with an Eigenvalue > 1.0 were extracted and a varimax rotation was selected. Water maze results were also used as an endpoint in the dedicated manuscript on serial TSPO-PET in both cohorts (Biechele et al., 2022). For immunohistochemistry quantifications GraphPad Prism (GraphPad Software, San Diego, California, United States) was used. All analyses were performed by an operator blinded to the experimental conditions. Data were normally distributed according to Shapiro-Wilk or D'Agostino-Pearson test. One-way analysis of variance (ANOVA) including Bonferroni *post-hoc* correction was used for group comparisons > 2 subgroups. For assessment of inter-group differences at single time points, Student's *t*-test (unpaired, two-sided) was applied. All results are presented as mean \pm SEM. *P*-values < 0.05 are defined as statistically significant.

RESULTS

Long-Term Pioglitazone Treatment Provokes a Significant Increase of the A β -PET Signal in PS2APP Mice

First, we analyzed serial changes of fibrillar amyloidosis under chronic pioglitazone treatment by [18 F]florbetaben A β -PET in PS2APP mice and wild-type controls. Vehicle treated PS2APP mice showed an elevated A β -PET SUVR when compared to vehicle treated wild-type at 8 (+20.4%, $p < 0.0001$) and 13 months of age (+37.9%, $p < 0.0001$). As expected, the A β -PET SUVR of wild-type mice did not change between 8 and 13 months of age (0.831 ± 0.003 vs. 0.827 ± 0.008 ; $p = 0.645$). Surprisingly, pioglitazone treatment provoked a stronger longitudinal increase in the A β -PET signal of PS2APP mice (+21.4%) when compared to vehicle treated PS2APP mice (+14.1%, $p = 0.002$). At the follow-up time point, the A β -PET SUVR was significantly elevated when compared to untreated PS2APP mice (**Figure 1**; 1.140 ± 0.014 vs. 1.187 ± 0.011 ; $p = 0.0017$). Pioglitazone treatment in wild-type mice provoked no changes of A β -PET SUVR compared to vehicle-treated wild-type mice at the follow-up time-point (0.827 ± 0.008 vs. 0.823 ± 0.005 ; $p = 0.496$; for images of wild-type mice see **Supplementary Figure 1**). Taken together, we found a significant increase in the A β -PET signal, which implied an increase in fibrillary A β -levels under pioglitazone treatment in PS2APP mice.

A β -PET Detects a Strong Increase of the Fibrillar A β -Load in *App*^{NL-G-F} Mice During Chronic PPAR γ Stimulation

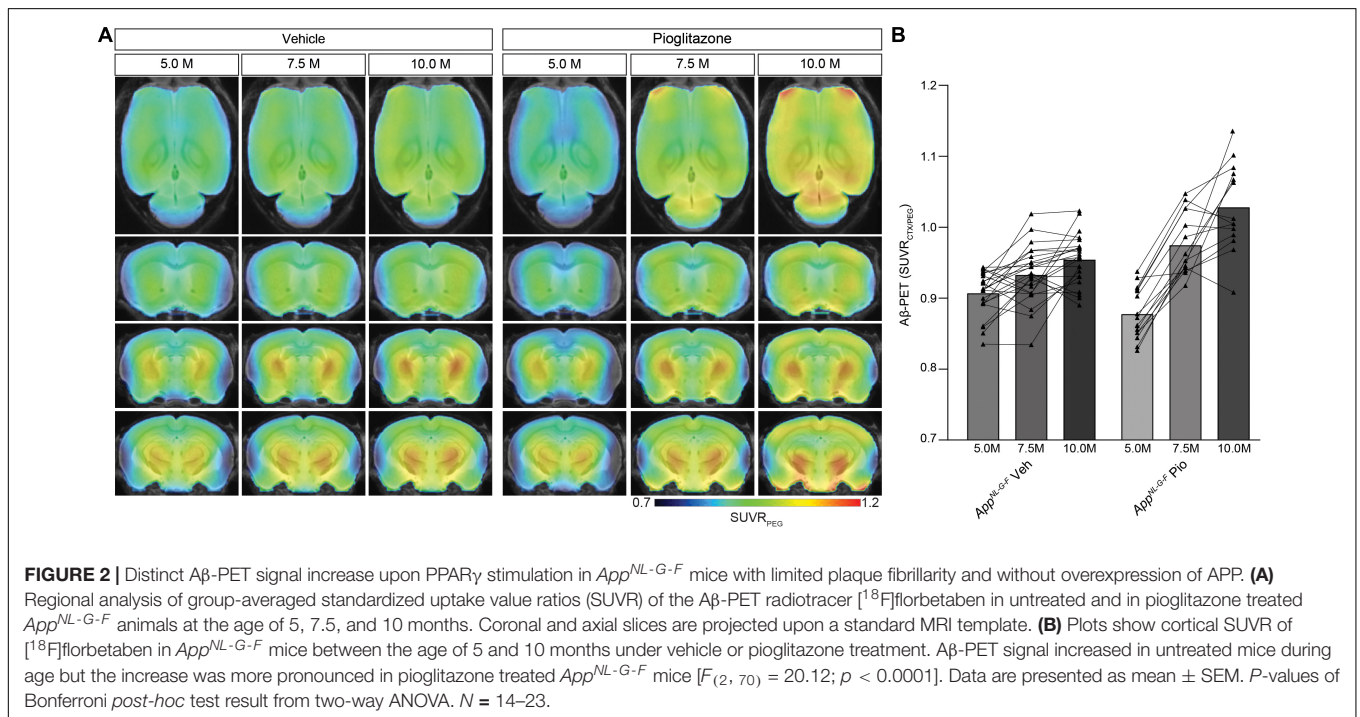
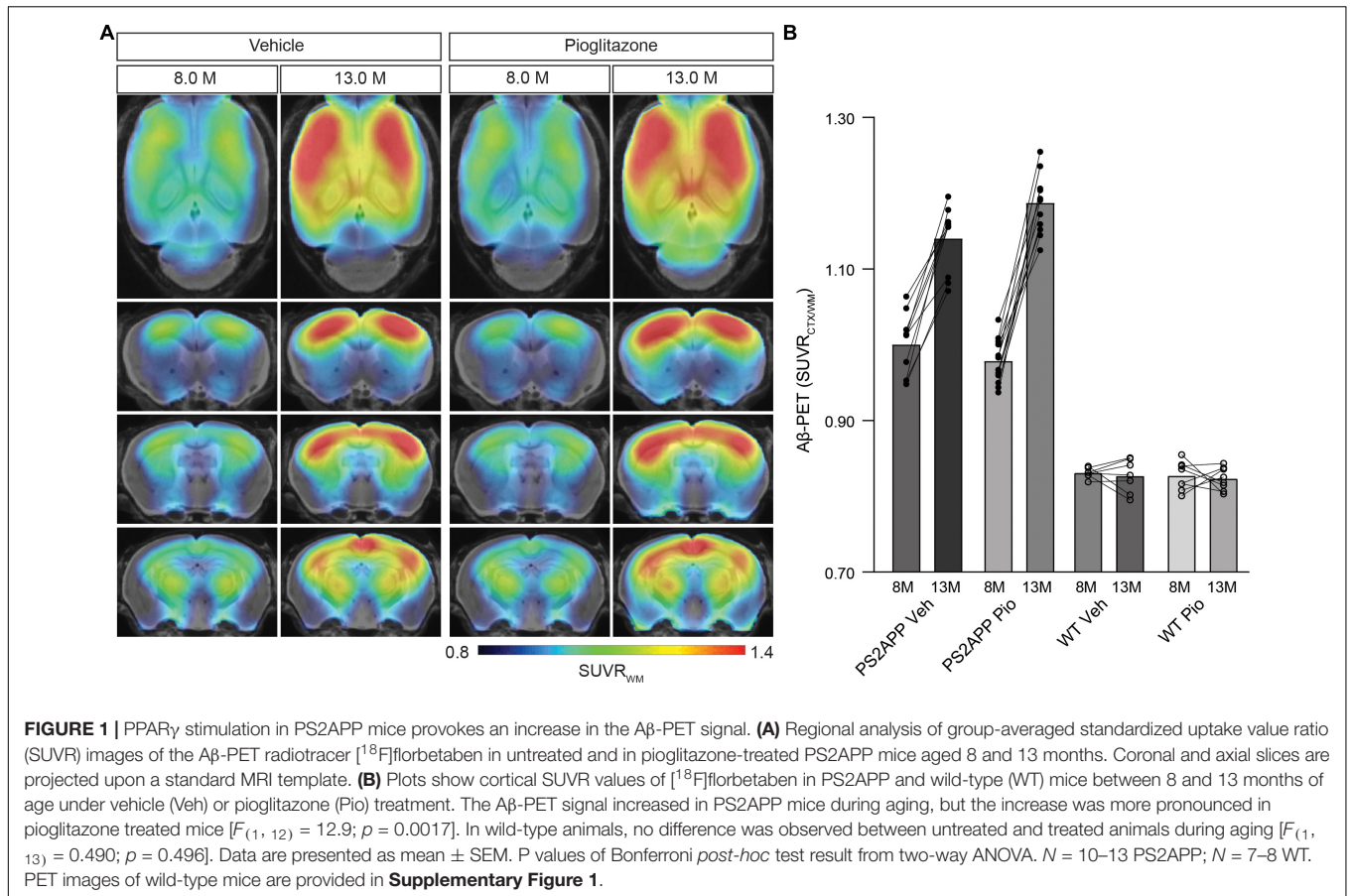
Next, we sought to validate our unexpected findings in PS2APP mice a mouse model with differing A β plaque composition, namely the *App*^{NL-G-F} mouse, which has limited fibrillarity due to endogenous expression of APP with three FAD mutations

(Saito et al., 2014). Strikingly, the effect of pioglitazone treatment on the A β -PET signal was even stronger in *App*^{NL-G-F} mice than in PS2APP mice. There was a pronounced increase of the A β -PET signal during chronic pioglitazone treatment (+17.2%) compared to vehicle (+5.3%, $p < 0.0001$). *App*^{NL-G-F} mice with pioglitazone treatment had a higher A β -PET SUVR at 7.5 (+4.6%, $p = 0.0071$) and 10 (+7.7%, $p < 0.0001$) months of age when compared to vehicle-treated *App*^{NL-G-F} mice (**Figure 2**). The baseline level of A β -PET SUVR was non-significantly lower in treated compared to untreated *App*^{NL-G-F} mice (0.878 ± 0.010 vs. 0.906 ± 0.006 , $p = 0.1350$). In both mouse models, the A β -signal increase after pioglitazone-treatment compared to baseline scans was pronounced in the frontotemporal cortex and hippocampal area (**Figures 1A, 2A**). In summary, the pioglitazone treatment augmented the A β -PET signal increase in both mouse models; this unexpected result was more pronounced in the *App*^{NL-G-F} model, which expresses less fibrillary A β plaques.

Pioglitazone Triggers A Shift Toward Increased A β -Plaque Fibrillarity in Two Distinct Mouse Models of Amyloidosis

Given the unexpected *in vivo* findings, we set about to evaluate the molecular correlates of the potentiation of A β -PET signal during pioglitazone treatment in AD model mice. The (immuno)histochemical analysis showed that the observed increase of the A β -PET signal was predominantly explicable by a change in plaque composition rather than by a change in plaque density (**Figure 3**). In both mouse models, the proportion of fibrillary A β stained with methoxy-X04 increased significantly under pioglitazone treatment compared to vehicle treated animals (PS2APP: $29.6 \pm 3.5\%$ vs. $15.2 \pm 0.7\%$, $p = 0.0056$, **Figure 3C**; *App*^{NL-G-F}: $9.1 \pm 1.6\%$ vs. $4.4 \pm 0.4\%$, $p = 0.0001$, **Figure 3D**). Pioglitazone treatment had no significant effect on the proportion of pre-fibrillary A β stained with NAB228 in PS2APP mice (PS2APP: $65.4 \pm 6.1\%$ vs. $67.0 \pm 6.9\%$, $p = 0.865$, **Figure 3C**). In *App*^{NL-G-F} mice, however, the proportion of pre-fibrillary A β decreased significantly in treated animals (*App*^{NL-G-F}: $26.7 \pm 1.7\%$ vs. $34.5 \pm 1.7\%$, $p = 0.0138$, **Figure 3E**). The effect size of pioglitazone treatment on plaque morphology was larger in *App*^{NL-G-F} mice than in PS2APP mice, which was reflected by a significantly increased overlay of methoxy-X04 and NAB228 positive plaques proportions in relation to untreated mice (PS2APP: $40.4 \pm 3.6\%$ vs. $25.1 \pm 2.1\%$, $p = 0.0075$, **Figure 3C**; *App*^{NL-G-F}: $35.0 \pm 3.4\%$ vs. $12.9 \pm 1.3\%$, $p = 0.0005$, **Figure 3E**). We attribute this effect to the generally diffuse nature of the plaque composition of *App*^{NL-G-F} mice, which predominantly contain high oligomeric and low fibrillary fractions of A β (Monasor et al., 2020) (compare **Figures 3A,B**).

The number of methoxy positive A β -plaques were similar between vehicle and pioglitazone treated groups for PS2APP ($1,016 \pm 107$ vs. $1,118 \pm 121$, $p = 0.547$, **Figure 3D**) and *App*^{NL-G-F} mice (242 ± 56 vs. 266 ± 33 , $p = 0.722$, **Figure 3F**). Notably there was no significant effect of chronic pioglitazone treatment on the different insoluble A β species (A β 40, A β 42) as well as on the level of the soluble A β 42-isoform observed in



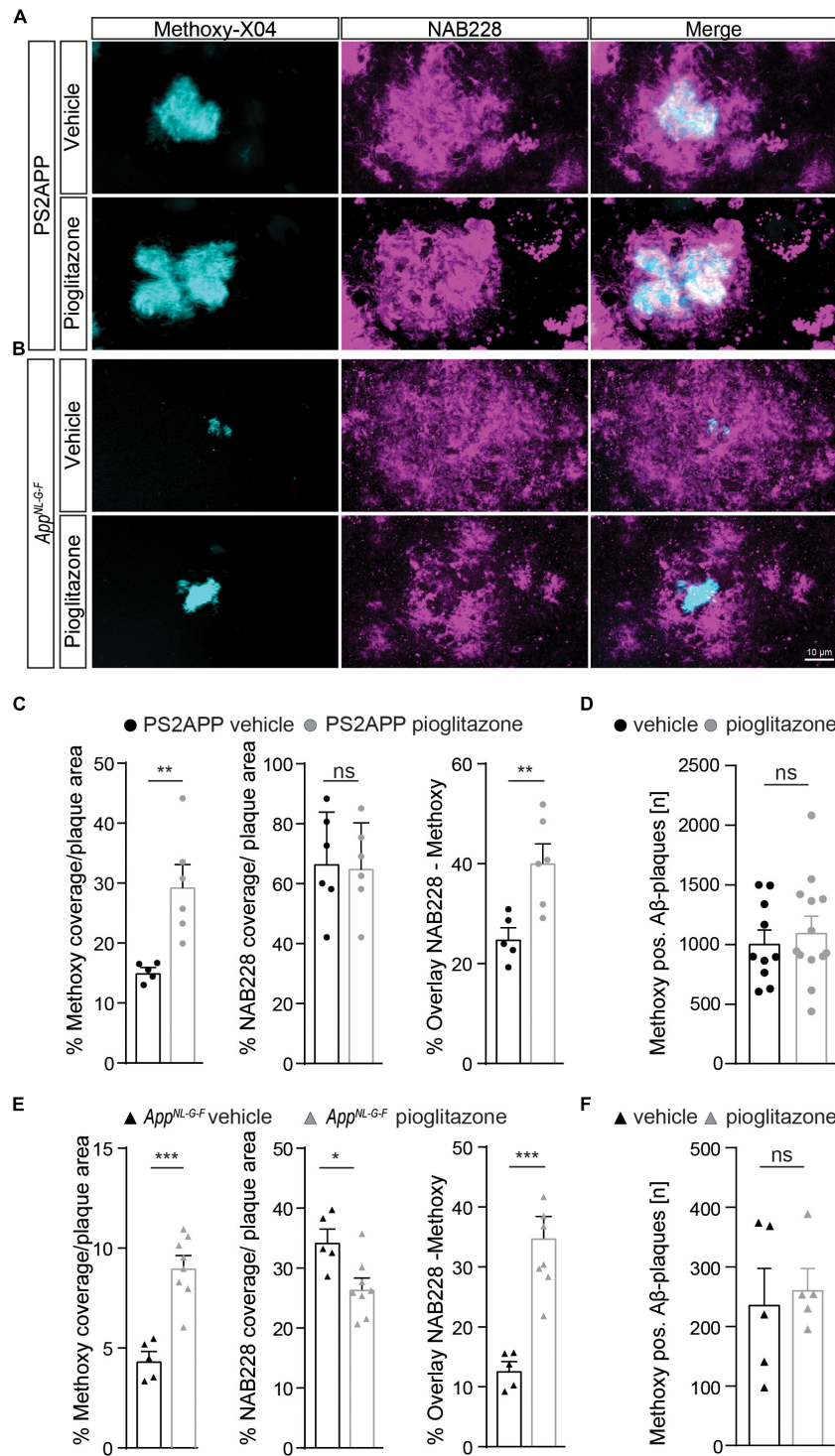


FIGURE 3 | Pioglitazone treatment triggers a change in plaque composition in two different mouse models of amyloidosis. Staining of fibrillary A β (methoxy-X04, cyan) and pre-fibrillary A β (NAB228, magenta) in vehicle and pioglitazone treated PS2APP mice **(A)** and *App^{NL-G-F}* mice **(B)**. **(C)** The plaque area covered by methoxy-X04 staining was significantly higher [$t_{(9)} = 3.612$; $p = 0.0056$], whereas the plaque area covered by NAB228 staining remained equal [$t_{(10)} = 0.175$; $p = 0.865$] in pioglitazone treated PS2APP mice. The overlay of NAB228 and methoxy staining increased under pioglitazone treatment [$t_{(9)} = 3.432$; $p = 0.0075$]. **(D)** The number of methoxy positive A β -plaques did not change under pioglitazone treatment in PS2APP-mice. **(E)** In *App^{NL-G-F}* mice, methoxy coverage [$t_{(11)} = 5.802$; $p = 0.0001$], NAB228 coverage [$t_{(11)} = 5.80$; $p = 0.0001$], as well as the overlay of both staining [$t_{(11)} = 2.93$; $p = 0.0138$], increased under pioglitazone treatment. **(F)** In *App^{NL-G-F}* mice, the number of methoxy positive A β -plaques did not change under pioglitazone. Data are presented as mean \pm SEM; $n = 5$ –13 mice. Two-sample student's *t*-test results: * $p < 0.05$; ** $p < 0.01$; *** $p < 0.001$.

either mouse model (**Supplementary Figure 2**). Taken together, our results indicate that the potentiated increase of the A β -PET signal upon pioglitazone treatment reflected a change in plaque composition from less dense pre-fibrillar amyloid aggregates to fibrillary A β -fractions.

Microglial Activation Is Reduced Upon PPAR γ Stimulation in Both Alzheimer's Disease Mouse Models

To confirm changes in the activation state of microglial cells, we performed Iba1 as well as CD68 immunohistochemical staining of activated microglia in both mouse models. We observed that pioglitazone treatment significantly decreased microglial activation in both mouse models (**Figure 4**). In PS2APP mice, PPAR γ stimulation provoked a one-third reduction of area coverage of Iba1-positive microglial cells (area: $9.1 \pm 0.6\%$) compared to untreated mice ($14.0 \pm 0.5\%$, $p = 0.0003$), and also a significant reduction of CD68-positive microglial cells area ($7.6 \pm 0.4\%$ vs. $9.9 \pm 0.3\%$, $p = 0.0018$). In pioglitazone treated *App^{NL-G-F}* mice, the area reduction was less pronounced, but still significant for Iba1-positive microglial cells ($9.4 \pm 0.2\%$ vs. $10.6 \pm 0.2\%$, $p = 0.0015$) and CD68-positive microglial cells ($2.7 \pm 0.1\%$ vs. $3.0 \pm 0.1\%$, $p = 0.0141$) compared to untreated mice. Thus, we observed a consistent net reduction of activated microglial coverage in both models; the lesser effect in *App^{NL-G-F}* mice might indicate partial compensation by triggering of microglial activation due to increased fibrillary A β levels (Sebastian et al., 2020).

Cognitive Function Is Improved by Chronic Pioglitazone Treatment in Association With an Increasing A β -PET Rate of Change

Finally, we aimed to elucidate whether the observed longitudinal changes in the composition of A β -plaques affected synaptic density and hippocampus related cognitive performance.

In PS2APP mice, treatment with pioglitazone resulted in a significant reduction of the water maze performance index compared to untreated mice during the probe trial (**Figure 5A**; $p = 0.0155$), whereas in wild-type animals there was no difference between treated and untreated animals ($p > 0.999$). The water maze performance index of pioglitazone treated PS2APP mice correlated strongly with the rate of increase in A β -PET signal (**Figure 5C**; $R = 0.686$; $p = 0.0097$). In *App^{NL-G-F}* mice, pioglitazone treatment did not result in a significant change of spatial learning performance (**Figure 5B**; $p > 0.999$). Accordingly, the water maze performance index and the rate of change in the A β -PET signal of pioglitazone treated *App^{NL-G-F}* mice did not correlate significantly (**Figure 5D**; $R = 0.341$; $p = 0.254$). There was no significant association between the water maze performance index and the A β -PET rate of change in vehicle treated PS2APP or *App^{NL-G-F}* mice.

To explore the basis of water maze results in PS2APP mice at the molecular level, we performed staining of synaptic density in the hippocampus. A β -oligomers are the primary neurotoxic forms of A β , while A β -fibrils have less neurotoxicity

(Hardy and Selkoe, 2002; Haass and Selkoe, 2007; Zott et al., 2019). Thus, we hypothesized that pre-synaptic density in the hippocampal CA1-Area would be rescued upon pioglitazone-treatment. In wild-type mice we did not observe altered changed VGLUT1 density under pioglitazone treatment (**Figure 5E, F**; 0.519 ± 0.007 1/ μm vs. 0.502 ± 0.008 1/ μm , $p = 0.810$). In PS2APP mice, however, we found that pioglitazone treatment significantly rescued spine density in the CA1-region of the hippocampus compared to untreated animals (**Figures 5E,F**; 0.497 ± 0.006 1/ μm vs. 0.459 ± 0.007 1/ μm , $p = 0.0012$), supporting the hippocampal-dependent water maze results.

DISCUSSION

To our knowledge, this is the first large-scale longitudinal PET study of cerebral A β -deposition in two distinct AD mouse models treated with the PPAR γ agonist pioglitazone. We combined *in vivo* PET monitoring with behavioral testing and detailed immunohistochemical analysis. Our main finding was an unexpected potentiation in both mouse models of the increasing A β -PET signal during 5 months of pioglitazone treatment. This increase occurred despite an improvement of spatial learning and prevention of synaptic loss in the PS2APP mice. Immunohistochemistry revealed a shift toward plaque composition of higher fibrillarity as the molecular correlate of the A β -PET signal in both mouse models. In PS2APP mice this increase was directly associated with improved cognitive performance, whereas in *App^{NL-G-F}* mice such an effect was not observed.

A β -PET enables longitudinal *in vivo* detection of A β -plaques, which plays an important role in AD diagnosis, monitoring disease progression, and as an endpoint for therapeutic treatment effects (Valotassiou et al., 2018). In our preceding observational and interventional studies, we validated in AD model mice the clinically established A β -PET tracer [^{18}F]florbetaben relative to histologically defined indices A β deposition (Brendel et al., 2015a,b). So far, an enhanced or increasing [^{18}F]florbetaben-PET signal has been interpreted as an indicator of disease progression or treatment failure (Laforce et al., 2018). Unexpectedly, we found that pioglitazone potentiated the increasing A β -PET signal in two mouse models compared to vehicle controls; in both cases, this increase was due to a shift of the plaque composition toward higher fibrillarity, and away from the more neurotoxic oligomeric form. However, ELISA measurements of plaque associated fibrillary A β extracted with formic acid did not indicate a change in the A β species composition in brain. This suggests that A β -PET imaging and immunohistochemical analysis detect treatment effects on A β -plaque composition that do not arise from a shift in the levels of A β species, and which may thus evade detection in studies of CSF or plasma content (Hansson et al., 2018).

Furthermore, our study provides evidence that rescued spatial learning deficits and prevented hippocampal synaptic loss can occur despite an increasing A β -PET signal upon immunomodulation. The combined results might sound contradictory, but according to the amyloid cascade hypothesis,

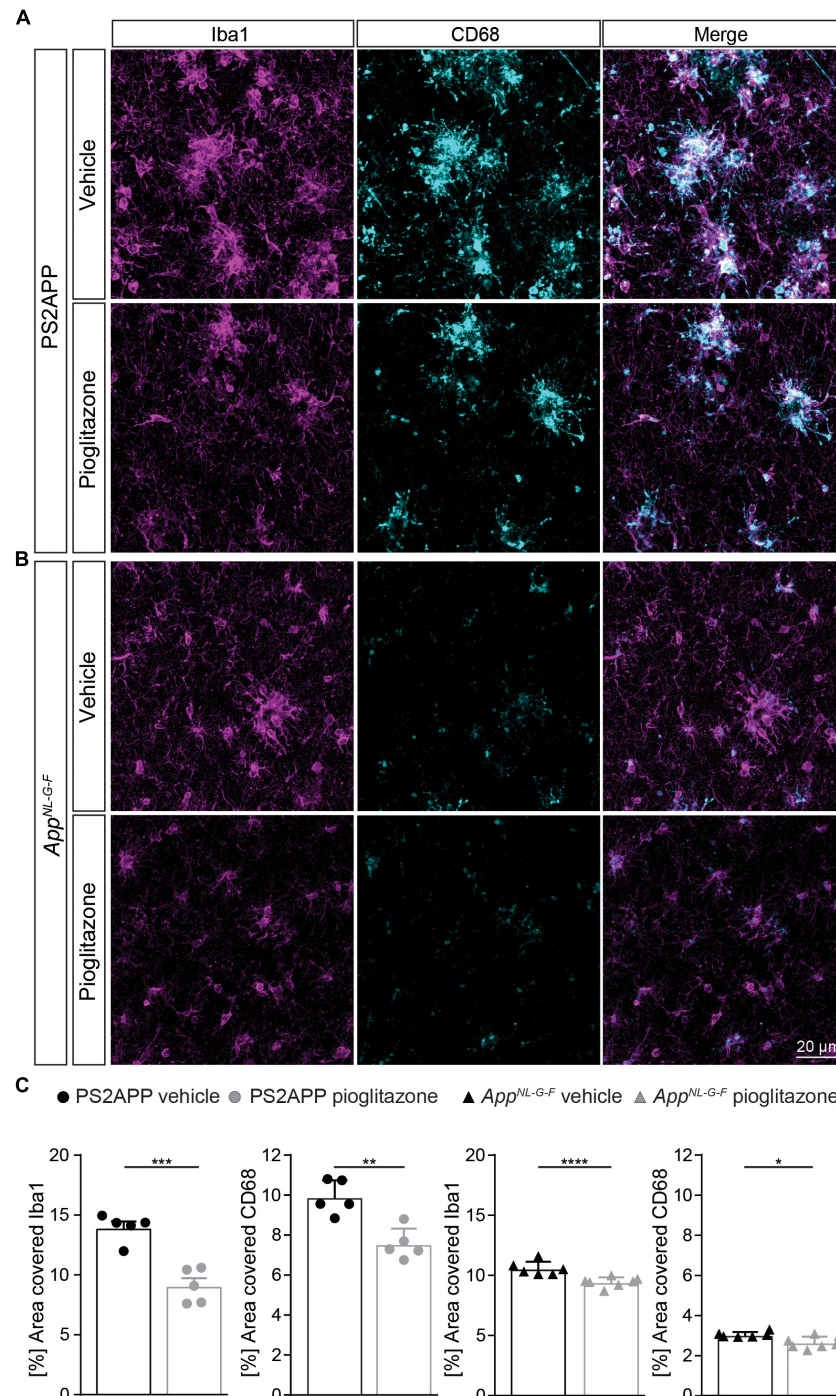
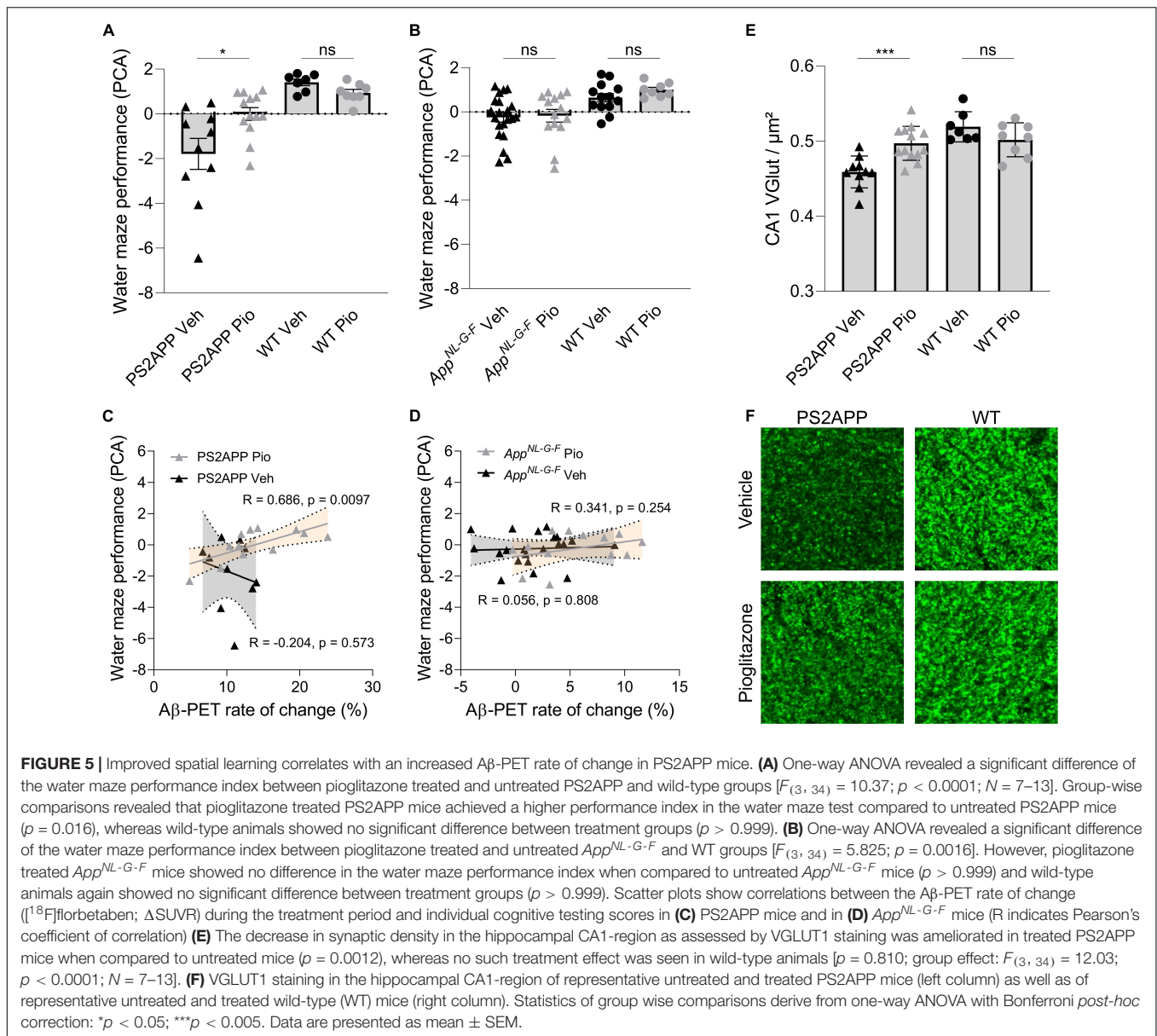


FIGURE 4 | Pioglitazone treatment reduces microglial activation in both AD mouse models. Iba1- (magenta) as well as CD68-(cyan) positive microglial cells in PS2APP **(A)** and *App*^{NL-G-F} mice **(B)**. **(C)** The area of Iba1 positive microglial cells [$t_{(8)} = 5.95$; $p = 0.0003$] as well as CD68 positive microglial cells [$t_{(8)} = 4.58$; $p = 0.0018$] decreased in treated PS2APP mice. The same effect was observed in *App*^{NL-G-F} mice where the area covered by Iba1 positive [$t_{(11)} = 4.21$; $p = 0.0015$] as well as CD68 positive microglial cells [$t_{(11)} = 2.91$; $p = 0.014$] were significantly reduced in treated compared to untreated mice. Data are presented as mean \pm SEM; $n = 5-7$ mice. Two-sample student's *t*-test results: * $p < 0.05$; ** $p < 0.01$; **** $p < 0.0001$.

A β -oligomers rather than A β -fibrils are the neurotoxic A β -forms (Haass and Selkoe, 2007; Selkoe and Hardy, 2016). Indeed, high concentrations of A β -oligomers isolated from brain of AD

patients correlated significantly with the degree of cognitive impairment prior to death (Lue et al., 1999; McLean et al., 1999; Wang et al., 1999). Furthermore, A β -oligomers have been shown



to disrupt long-term potentiation at synapses and provoke long-term depression (Cullen et al., 1997; Hu et al., 2008; Klyubin et al., 2014). Thus, improved spatial learning and rescued synaptic density could reflect a therapeutically induced shift of A β to hypercondensed plaques, in keeping with observations of greater neuritic damage in association with more diffuse plaques (Ulrich et al., 2014; Wang et al., 2016). Furthermore, strongly in line with our present data, a recent study argued that microglia promoted formation of dense-core plaques may play a protective role in AD (Huang et al., 2021).

The shift in plaque composition was more pronounced in *App^{NL-G-F}* mice than in the PS2APP model. Due to the expression of the Arctic mutation (Saito et al., 2014), the A β -deposits of the *App^{NL-G-F}* line consist predominantly of A β -oligomers (Sacher et al., 2019; Monasor et al., 2020).

However, we observed no improvement in cognition in the APP knock-in mouse line after pioglitazone treatment. We attribute the lacking improvement of spatial learning to the minor deterioration of this model in water maze assessment at 10 months of age (Masuda et al., 2016; Sacher et al., 2019). Our present observation stand in contrast with previous studies showing that PPAR- γ agonists reduced A β -plaque formation by increasing A β -clearance (Camacho et al., 2004; Mandrekar-Colucci et al., 2012; Yamanaka et al., 2012). However, those studies only performed endpoint analyses, in part after short-term treatment of 9 days (Mandrekar-Colucci et al., 2012); the current work is the first to perform longitudinal *in vivo* monitoring of A β -deposition over a 5-month chronic PPAR- γ treatment period. We note that the divergent results could also reflect the different markers used for immunohistochemistry

compared to our present differentiated analysis of fibrillar and less dense pre-fibrillar A β components. As such, the decreased NAB228-positive plaque fraction in our treated *App^{NL-G-F}* mice fits to the earlier reported decrease of the 6E10-positive area in APPS1 mice (Mandrekar-Colucci et al., 2012). We note that the biochemical source of the A β -PET signal is still a matter of controversy, since some studies found no impact of non-fibrillar plaque components (Catafau et al., 2016) whereas others postulated a significant contribution of non-fibrillar A β to the A β -PET signal (Ikonovic et al., 2016, 2018, 2020). Recently, we were able to show that non-fibrillar components of A β plaques indeed contribute to the net A β -PET signal (Biechele et al., 2022). Therefore, increases in the [¹⁸F]florbetaben-PET signal must be precisely differentiated and interpreted with caution. Development of new PET tracers that selectively target oligomeric A β may realize a more precise discrimination of neurotoxic A β plaque manifestation (Schlin et al., 2016; Fang et al., 2019) and its impact on disease severity.

In line with previous pioglitazone studies (Mandrekar-Colucci et al., 2012; Yamanaka et al., 2012), we observed a decrease in microglial activity (Biechele et al., 2021), thus confirming the immunomodulatory effect of the drug. Since earlier studies have shown that fibrillary A β -deposits activate microglial cells (Sebastian et al., 2020) which then migrate toward the fibrillar deposits (Füger et al., 2017), resulting in an increased number of activated microglial cells surrounding A β -plaques (Blume et al., 2018), the inactivation and migration effects could cancel each other out. Based on our findings in both AD models, we conclude that, by increasing plaque fibrillarity, the immunomodulatory effect of pioglitazone overweighs the potential triggering of activated microglia. Modulating microglial phenotype to restore their salutogenic effects may prove crucial in new therapeutic trials (Lewcock et al., 2020). In several preclinical and clinical trials, pioglitazone proved to be a promising immunomodulatory approach for treatment of AD, especially in patients with comorbid diabetes (Liu et al., 2015; Cao et al., 2018). However, a large phase III trial of pioglitazone in patients with mild AD was discontinued due to lacking efficacy (Geldmacher et al., 2011). Our data calls for monitoring of the effects of PPAR γ agonists by A β -PET, which may help to stratify treatment responders based on their individual rates of A β plaque accumulation. Based on our results, we submit that personalized PPAR γ agonist treatment might be effective when the patient has capacity to successfully shift toxic pre-fibrillar A β toward fibrillar parts of the plaque.

We note as a limitation that PPAR γ receptor agonists represent a rather unspecific class of drugs since PPAR γ is involved in various pathways in addition to peroxisome activation, notably including glucose metabolism and insulin sensitization [48]. Future studies should address if the observed effects on A β plaque composition are also present for more selective immunomodulation strategies such as NLRP3 regulators [49]. Two different water maze examinations were performed in the present study due a switch of the laboratory. Hence, although we calculated a similar water maze performance index by a PCA of the main read-outs of each examination, the obtained results and the sensitivity to detect spatial learning deficits are not comparable between both A β mouse models.

CONCLUSION

In conclusion, chronic pioglitazone treatment provoked a longitudinal A β -PET signal increase in transgenic and knock-in mice due to a shift toward hypercondensed fibrillar A β plaques. The increasing rate of A β -PET signal increase with time was accompanied by ameliorated cognitive performance and attenuated synaptic loss after pioglitazone treatment. It follows that increasing A β -PET signal need not always indicate a treatment failure, since it is the composition of A β plaques that determines their neurotoxicity. In summary, our preclinical data indicate that a shift toward increasing fibrillar amyloidosis can be beneficial for the preservation of cognitive function and synaptic integrity.

DATA AVAILABILITY STATEMENT

The raw data supporting the conclusions of this article will be made available by the authors, without undue reservation.

ETHICS STATEMENT

The animal study was reviewed and approved by the Regierung von Oberbayern. Written informed consent was obtained from the owners for the participation of their animals in this study.

AUTHOR CONTRIBUTIONS

KB, HA, AR, PC, MW, MMD, JH, and MB conceived the study and analyzed the results. TB, MD, and MB wrote the manuscript with further input from all co-authors. MD, GB, CSC, KW, FE, CSa, and CF performed the small animal, PET experiments, and small animal PET data analyses. TB, FP, YS, KO, GK, XX, MMD, and JH performed immunohistochemistry experiments, analyses, and interpretation. F-JG and SL performed PET tracer synthesis and analyses. NF analyzed and interpreted serial PET data and contributed to their analysis. GB, BZ, KW, and HA performed spatial learning tests and interpretation. BU-S, KB, and MW supplied the study with animal models and interpreted the dedicated results. All authors contributed with intellectual content.

FUNDING

This study was supported by the FöFoLe Program of the Faculty of Medicine of the Ludwig Maximilian University, Munich (grant to MB). This work was funded by the Deutsche Forschungsgemeinschaft (DFG, German Research Foundation) to AR and MB—project numbers BR4580/1-1/RO5194/1-1. The work was supported by the Deutsche Forschungsgemeinschaft (DFG, German Research Foundation)

under Germany's Excellence Strategy within the framework of the Munich Cluster for Systems Neurology (EXC 2145 SyNergy—ID 390857198). MB was supported by the Alzheimer Forschung Initiative e.V (Grant No. 19063p).

ACKNOWLEDGMENTS

We thank Karin Bormann-Giglmaier and Rosel Oos for excellent technical assistance. Florbetaben precursor was provided by

REFERENCES

- Biechele, G., Blume, T., Deussing, M., Zott, B., Shi, Y., Xiang, X., et al. (2021). Chronic PPAR γ Stimulation Shifts Amyloidosis to Higher Fibrillarity but Improves Cognition. *bioRxiv* [Preprint]. doi: 10.1101/2021.05.30.446348
- Biechele, G., Monasor, L. S., Wind, K., Blume, T., Parhizkar, S., Arzberger, T., et al. (2022). Glitter in the Darkness? Non-fibrillar β -Amyloid Plaque Components Significantly Impact the β -Amyloid PET Signal in Mouse Models of Alzheimer Disease. *J. Nucl. Med.* 63, 117–124. doi: 10.2967/jnumed.120.261858
- Biechele, G., Wind, K., Blume, T., Sacher, C., Beyer, L., Eckenweber, F., et al. (2020). Microglial Activation in the Right Amygdala-Entorhinal-Hippocampal Complex is Associated with Preserved Spatial Learning in AppNL-G-F mice. *NeuroImage* 230:117707. doi: 10.1016/j.neuroimage.2020.117707
- Blume, T., Focke, C., Peters, F., Deussing, M., Albert, N. L., Lindner, S., et al. (2018). Microglial response to increasing amyloid load saturates with aging: a longitudinal dual tracer *in vivo* μ PET-study. *J. Neuroinflammation* 15:307. doi: 10.1186/s12974-018-1347-6
- Braak, H., and Braak, E. (1991). Neuropathological staging of Alzheimer-related changes. *Acta Neuropathol.* 82, 239–259. doi: 10.1007/BF00308809
- Brendel, M., Kleinberger, G., Probst, F., Jaworska, A., Overhoff, F., Blume, T., et al. (2017b). Increase of TREM2 during Aging of an Alzheimer's Disease Mouse Model Is Paralleled by Microglial Activation and Amyloidosis. *Front. Aging Neurosci.* 9:8. doi: 10.3389/fnagi.2017.00008
- Brendel, M., Focke, C., Blume, T., Peters, F., Deussing, M., Probst, F., et al. (2017a). Time Courses of Cortical Glucose Metabolism and Microglial Activity Across the Life Span of Wild-Type Mice: a PET Study. *J. Nucl. Med.* 58, 1984–1990. doi: 10.2967/jnumed.117.195107
- Brendel, M., Jaworska, A., Griefinger, E., Rötzer, C., Burgold, S., Gildehaus, F. J., et al. (2015a). Cross-sectional comparison of small animal [18F]-florbetaben amyloid-PET between transgenic AD mouse models. *PLoS One* 10:e0116678. doi: 10.1371/journal.pone.0116678
- Brendel, M., Jaworska, A., Herms, J., Trambauer, J., Rötzer, C., Gildehaus, F.-J., et al. (2015b). Amyloid-PET predicts inhibition of de novo plaque formation upon chronic γ -secretase modulator treatment. *Mol. Psychiatry* 20, 1179–1187. doi: 10.1038/mp.2015.74
- Brendel, M., Probst, F., Jaworska, A., Overhoff, F., Korzhova, V., Albert, N. L., et al. (2016). Glial Activation and Glucose Metabolism in a Transgenic Amyloid Mouse Model: a Triple-Tracer PET Study. *J. Nucl. Med.* 57, 954–960. doi: 10.2967/jnumed.115.167858
- Bromley-Brits, K., Deng, Y., and Song, W. (2011). Morris water maze test for learning and memory deficits in Alzheimer's disease model mice. *J. Vis. Exp.* 53:2920. doi: 10.3791/2920
- Busche, M. A., Kekuš, M., Adelsberger, H., Noda, T., Förstl, H., Nelken, I., et al. (2015). Rescue of long-range circuit dysfunction in Alzheimer's disease models. *Nat. Neurosci.* 18, 1623–1630. doi: 10.1038/nn.4137
- Camacho, I. E., Serneels, L., Spittaels, K., Merchiers, P., Dominguez, D., and De, S. B. (2004). Peroxisome-proliferator-activated receptor gamma induces a clearance mechanism for the amyloid-beta peptide. *J. Neurosci.* 24, 10908–10917. doi: 10.1523/JNEUROSCI.3987-04.2004
- Cao, B., Rosenblat, J. D., Brietzke, E., Park, C., Lee, Y., Musial, N., et al. (2018). Comparative efficacy and acceptability of antidiabetic agents for Alzheimer's disease and mild cognitive impairment: a systematic review and network meta-analysis. *Diabetes Obes. Metab.* 20, 2467–2471. doi: 10.1111/dom.13373
- Catafau, A. M., Bullich, S., Seibyl, J. P., Barthel, H., Ghetti, B., Leverenz, J., et al. (2016). Cerebellar Amyloid- β Plaques: how Frequent Are They, and Do They

Piramal Imaging. We thank Takashi Saito and Takaomi C. Saido for providing the App^{NL-G-F} mice.

SUPPLEMENTARY MATERIAL

The Supplementary Material for this article can be found online at: <https://www.frontiersin.org/articles/10.3389/fnagi.2022.854031/full#supplementary-material>

- Influence 18F-Florbetaben SUV Ratios? *J. Nucl. Med.* 57, 1740–1745. doi: 10.2967/jnumed.115.171652
- Cheng, H., Shang, Y., Jiang, L., Shi, T., and Wang, L. (2016). The peroxisome proliferators activated receptor-gamma agonists as therapeutics for the treatment of Alzheimer's disease and mild-to-moderate Alzheimer's disease: a meta-analysis. *Int. J. Neurosci.* 126, 299–307. doi: 10.3109/00207454.2015.1015722
- Cullen, W. K., Suh, Y. H., Anwyl, R., and Rowan, M. J. (1997). Block of LTP in rat hippocampus *in vivo* by beta-amyloid precursor protein fragments. *Neuroreport* 8, 3213–3217. doi: 10.1097/00001756-199710200-00006
- Dorostkar, M. M., Dreosti, E., Odermatt, B., and Lagnado, L. (2010). Computational processing of optical measurements of neuronal and synaptic activity in networks. *J. Neurosci. Methods* 188, 141–150. doi: 10.1016/j.jneumeth.2010.01.033
- Dorr, A., Sled, J. G., and Kabani, N. (2007). Three-dimensional cerebral vasculature of the CBA mouse brain: a magnetic resonance imaging and micro computed tomography study. *NeuroImage* 35, 1409–1423. doi: 10.1016/j.neuroimage.2006.12.040
- Fang, X. T., Hultqvist, G., Meier, S. R., Antoni, G., Sehlin, D., and Syvänen, S. (2019). High detection sensitivity with antibody-based PET radioligand for amyloid beta in brain. *NeuroImage* 184, 881–888. doi: 10.1016/j.neuroimage.2018.10.011
- Focke, C., Blume, T., Zott, B., Shi, Y., Deussing, M., Peters, F., et al. (2019). Early and Longitudinal Microglial Activation but Not Amyloid Accumulation Predicts Cognitive Outcome in PS2APP Mice. *J. Nucl. Med.* 60, 548–554. doi: 10.2967/jnumed.118.217703
- Füger, P., Hefendehl, J. K., Veeraraghavalu, K., Wendeln, A. C., Schlosser, C., Obermüller, U., et al. (2017). Microglia turnover with aging and in an Alzheimer's model *via* long-term *in vivo* single-cell imaging. *Nat. Neurosci.* 20, 1371–1376. doi: 10.1038/nn.4631
- Geldmacher, D. S., Fritsch, T., McClendon, M. J., and Landreth, G. (2011). A randomized pilot clinical trial of the safety of pioglitazone in treatment of patients with Alzheimer disease. *Arch. Neurol.* 68, 45–50. doi: 10.1001/archneurol.2010.229
- Haass, C., and Selkoe, D. J. (2007). Soluble protein oligomers in neurodegeneration: lessons from the Alzheimer's amyloid β -peptide. *Nat. Rev. Mol. Cell Biol.* 8, 101–112. doi: 10.1038/nrm2101
- Hansson, O., Seibyl, J., Stomrud, E., Zetterberg, H., Trojanowski, J. Q., Bittner, T., et al. (2018). CSF biomarkers of Alzheimer's disease concord with amyloid- β PET and predict clinical progression: a study of fully automated immunoassays in BioFINDER and ADNI cohorts. *Alzheimers Dement.* 14, 1470–1481. doi: 10.1016/j.jalz.2018.01.010
- Hardy, J., and Selkoe, D. J. (2002). The amyloid hypothesis of Alzheimer's disease: progress and problems on the road to therapeutics. *Science* 297, 353–356. doi: 10.1126/science.1072994
- Heneka, M. T., Carson, M. J., Khoury, J. E., Landreth, G. E., Brosseron, F., Feinstein, D. L., et al. (2015). Neuroinflammation in Alzheimer's disease. *Lancet Neurol.* 14, 388–405. doi: 10.1016/S1474-4422(15)70016-5
- Heppner, F. L., Ransohoff, R. M., and Becher, B. (2015). Immune attack: the role of inflammation in Alzheimer disease. *Nature reviews. Neuroscience* 16, 358–372. doi: 10.1038/nrn3880
- Hickman, S. E., Allison, E. K., and El Khoury, J. (2008). Microglial Dysfunction and Defective β -Amyloid Clearance Pathways in Aging Alzheimer's Disease Mice. *J. Neurosci.* 28, 8354–8360. doi: 10.1523/JNEUROSCI.0616-08.2008

- Hu, N. W., Smith, I. M., Walsh, D. M., and Rowan, M. J. (2008). Soluble amyloid-beta peptides potentially disrupt hippocampal synaptic plasticity in the absence of cerebrovascular dysfunction *in vivo*. *Brain* 131, 2414–2424. doi: 10.1093/brain/awn174
- Huang, Y., Happonen, K. E., Burrola, P. G., O'Connor, C., Hah, N., Huang, L., et al. (2021). Microglia use TAM receptors to detect and engulf amyloid β plaques. *Nat. Immunol.* 22, 586–594. doi: 10.1038/s41590-021-00913-5
- Ikonomic, M. D., Buckley, C. J., Abrahamson, E. E., Kofler, J. K., Mathis, C. A., Klunk, W. E., et al. (2020). Post-mortem analyses of PiB and flutemetamol in diffuse and cored amyloid- β plaques in Alzheimer's disease. *Acta Neuropathol.* 140, 463–476. doi: 10.1007/s00401-020-02175-1
- Ikonomic, M. D., Buckley, C. J., Heurling, K., Sherwin, P., Jones, P. A., Zanette, M., et al. (2016). Post-mortem histopathology underlying β -amyloid PET imaging following flutemetamol F 18 injection. *Acta Neuropathol. Commun.* 4:130. doi: 10.1186/s40478-016-0399-z
- Ikonomic, M. D., Fantoni, E. R., Farrar, G., and Salloway, S. (2018). Infrequent false positive [18 F]flutemetamol PET signal is resolved by combined histological assessment of neuritic and diffuse plaques. *Alzheimers Res. Ther.* 10, 1–4. doi: 10.1186/s13195-018-0387-6
- Keskin, A. D., Kekuš, M., Adelsberger, H., Neumann, U., Shimshek, D. R., Song, B., et al. (2017). BACE inhibition-dependent repair of Alzheimer's pathophysiology. *Proc. Natl. Acad. Sci. U. S. A.* 114, 8631–8636. doi: 10.1073/pnas.1708106114
- Klyubin, I., Ondrejčák, T., Hayes, J., Cullen, W. K., Mably, A. J., Walsh, D. M., et al. (2014). Neurotransmitter receptor and time dependence of the synaptic plasticity disrupting actions of Alzheimer's disease A β *in vivo*. *Philos. Trans. R. Soc. Lond. B Biol. Sci.* 369:20130147. doi: 10.1098/rstb.2013.0147
- Laforce, R., Soucy, J.-P., Sellami, L., Dallaire-Thérault, C., Brunet, F., Bergeron, D., et al. (2018). Molecular imaging in dementia: past, present, and future. *Alzheimers Dement.* 14, 1522–1552. doi: 10.1016/j.jalz.2018.06.2855
- Lee, C. Y., and Landreth, G. E. (2010). The role of microglia in amyloid clearance from the AD brain. *J. Neural Transm.* 117, 949–960. doi: 10.1007/s00702-010-0433-4
- Lewcock, J. W., Schlepckow, K., Di Paolo, G., Tahirovic, S., Monroe, K. M., and Haass, C. (2020). Emerging Microglia Biology Defines Novel Therapeutic Approaches for Alzheimer's Disease. *Neuron* 108, 801–821. doi: 10.1016/j.neuron.2020.09.029
- Liu, J., Wang, L. N., and Jia, J. P. (2015). Peroxisome proliferator-activated receptor-gamma agonists for Alzheimer's disease and amnesic mild cognitive impairment: a systematic review and meta-analysis. *Drugs Aging* 32, 57–65. doi: 10.1007/s40266-014-0228-7
- Lue, L.-F., Kuo, Y.-M., Roher, A. E., Brachova, L., Shen, Y., Sue, L., et al. (1999). Soluble Amyloid β Peptide Concentration as a Predictor of Synaptic Change in Alzheimer's Disease. *Am. J. Pathol.* 155, 853–862. doi: 10.1016/s0002-9440(10)65184-x
- Mandrekar-Colucci, S., Karlo, J. C., and Landreth, G. E. (2012). Mechanisms Underlying the Rapid Peroxisome Proliferator-Activated Receptor- γ -Mediated Amyloid Clearance and Reversal of Cognitive Deficits in a Murine Model of Alzheimer's Disease. *J. Neurosci.* 32, 10117–10128. doi: 10.1523/JNEUROSCI.5268-11.2012
- Manook, A., Yousefi, B. H., Willuweit, A., Platzer, S., Reder, S., Voss, A., et al. (2012). Small-Animal PET Imaging of Amyloid-Beta Plaques with [11C]PiB and Its Multi-Modal Validation in an APP/PS1 Mouse Model of Alzheimer's Disease. *PLoS One* 7:e31310. doi: 10.1371/journal.pone.0031310
- Masuda, A., Kobayashi, Y., Kogo, N., Saito, T., Saido, T. C., and Itohara, S. (2016). Cognitive deficits in single App knock-in mouse models. *Neurobiol. Learn. Mem.* 135, 73–82. doi: 10.1016/j.nlm.2016.07.001
- McLean, C. A., Cherny, R. A., Fraser, F. W., Fuller, S. J., Smith, M. J., Beyreuther, K., et al. (1999). Soluble pool of Abeta amyloid as a determinant of severity of neurodegeneration in Alzheimer's disease. *Ann. Neurol.* 46, 860–866. doi: 10.1002/1531-8249(199912)46:6<860::aid-ana8>3.0.co;2-m doi: 10.1002/1531-8249(199912)46:6
- Monasor, L. S., Müller, S. A., Colombo, A. V., Tanriover, G., König, J., Roth, S., et al. (2020). Fibrillar A β triggers microglial proteome alterations and dysfunction in Alzheimer mouse models. *eLife* 9:e54083 doi: 10.7554/eLife.54083
- Moon, J. H., Kim, H. J., Yang, A. H., Kim, H. M., Lee, B.-W., Kang, E. S., et al. (2012). The effect of rosiglitazone on LRP1 expression and amyloid β uptake in human brain microvascular endothelial cells: a possible role of a low-dose thiazolidinedione for dementia treatment. *Int. J. Neuropsychopharmacol.* 15, 135–142. doi: 10.1017/S1461145711001611
- Overhoff, F., Brendel, M., Jaworska, A., Korzhova, V., Delker, A., Probst, F., et al. (2016). Automated Spatial Brain Normalization and Hindbrain White Matter Reference Tissue Give Improved [18F]-Florbetaben PET Quantitation in Alzheimer's Model Mice. *Front. Neurosci.* 10:45. doi: 10.3389/fnins.2016.00045
- Ozmen, L., Albentz, A., Czech, C., and Jacobsen, H. (2008). Expression of Transgenic APP mRNA Is the Key Determinant for Beta-Amyloid Deposition in PS2APP Transgenic Mice. *Neurodegener. Dis.* 6, 29–36. doi: 10.1159/000170884
- Page, R. M., Baumann, K., Tomioka, M., Pérez-Revuelta, B. I., Fukumori, A., Jacobsen, H., et al. (2008). Generation of Abeta38 and Abeta42 is independently and differentially affected by familial Alzheimer disease-associated presenilin mutations and gamma-secretase modulation. *J. Biol. Chem.* 283, 677–683. doi: 10.1074/jbc.M708754200
- Rominger, A., Brendel, M., Burgold, S., Keppler, K., Baumann, K., Xiong, G., et al. (2013). Longitudinal Assessment of Cerebral β -Amyloid Deposition in Mice Overexpressing Swedish Mutant β -Amyloid Precursor Protein Using 18F-Florbetaben PET. *J. Nucl. Med.* 54, 1127–1134. doi: 10.2967/jnumed.112.114660
- Sacher, C., Blume, T., Beyer, L., Peters, F., Eckenweber, F., Sgobio, C., et al. (2019). Longitudinal PET Monitoring of Amyloidosis and Microglial Activation in a Second-Generation Amyloid- β Mouse Model. *J. Nucl. Med.* 60, 1787–1793. doi: 10.2967/jnumed.119.227322
- Saito, T., Matsuba, Y., Mihira, N., Takano, J., Nilsson, P., Itohara, S., et al. (2014). Single App knock-in mouse models of Alzheimer's disease. *Nat. Neurosci.* 17, 661–663. doi: 10.1038/nn.3697
- Sasaguri, H., Nilsson, P., Hashimoto, S., Nagata, K., Saito, T., Strooper, B., et al. (2017). APP mouse models for Alzheimer's disease preclinical studies. *EMBO J.* 36, 2473–2487. doi: 10.15252/emboj.201797397
- Sauvage, M., Brabet, P., Holsboer, F., Bockaert, J., and Steckler, T. (2000). Mild deficits in mice lacking pituitary adenylate cyclase-activating polypeptide receptor type 1 (PAC1) performing on memory tasks. *Mol. Brain Res.* 84, 79–89. doi: 10.1016/S0169-328X(00)00219-9
- Sebastian, M. L., Müller, S. A., Colombo, A. V., Tanriover, G., König, J., Roth, S., et al. (2020). Fibrillar A β triggers microglial proteome alterations and dysfunction in Alzheimer mouse models. *eLife* 9:e54083.
- Sehlin, D., Fang, X. T., Cato, L., Antoni, G., Lannfelt, L., and Syvänen, S. (2016). Antibody-based PET imaging of amyloid beta in mouse models of Alzheimer's disease. *Nat. Commun.* 7:306. doi: 10.1038/ncomms10759
- Selkoe, D. J., and Hardy, J. (2016). The amyloid hypothesis of Alzheimer's disease at 25 years. *EMBO Mol. Med.* 8, 595–608. doi: 10.15252/emmm.201606210
- Streit, W. J., Xue, Q. S., Tischer, J., and Bechmann, I. (2014). Microglial pathology. *Acta Neuropathol. Commun.* 2, 1–17. doi: 10.1186/s40478-014-0142-6
- Ulrich, J. D., Finn, M. B., Wang, Y., Shen, A., Mahan, T. E., Jiang, H., et al. (2014). Altered microglial response to A β plaques in APPPS1-21 mice heterozygous for TREM2. *Mol. Neurodegener.* 9, 1–9. doi: 10.1186/1750-1326-9-20
- Valotassiou, V., Malamitsi, J., Papatrifaflou, J., Dardiotis, E., Tsougos, I., Psimadas, D., et al. (2018). SPECT and PET imaging in Alzheimer's disease. *Ann. Nucl. Med.* 32, 583–593. doi: 10.1007/s12149-018-1292-6
- Wang, J., Dickson, D. W., Trojanowski, J. Q., and Lee, V. M. (1999). The levels of soluble versus insoluble brain Abeta distinguish Alzheimer's disease from normal and pathologic aging. *Exp. Neurol.* 158, 328–337. doi: 10.1006/exnr.1999.7085
- Wang, Y., Ulland, T. K., Ulrich, J. D., Song, W., Tzaferis, J. A., Hole, J. T., et al. (2016). TREM2-mediated early microglial response limits diffusion and toxicity of amyloid plaques. *J. Exp. Med.* 213, 667–675. doi: 10.1084/jem.20151948
- Yamanaka, M., Ishikawa, T., Griep, A., Axt, D., Kummer, M. P., and Heneka, M. T. (2012). PPAR/RXR-Induced and CD36-Mediated Microglial Amyloid-Phagocytosis Results in Cognitive Improvement in Amyloid Precursor Protein/Presenilin 1 Mice. *J. Neurosci.* 32, 17321–17331. doi: 10.1523/JNEUROSCI.1569-12.2012
- Ziegler-Graham, K., Brookmeyer, R., Johnson, E., and Arrighi, H. M. (2008). Worldwide variation in the doubling time of Alzheimer's disease incidence rates. *Alzheimers Dement.* 4, 316–323. doi: 10.1016/j.jalz.2008.05.2479
- Zimmer, E., Leuzy, A., Benedet, A., Breitner, J., Gauthier, S., and Rosa-Neto, P. (2014). Tracking neuroinflammation in Alzheimer's disease: the role of positron

emission tomography imaging. *J. Neuroinflammation* 11:120. doi: 10.1186/1742-2094-11-120

Zott, B., Simon, M. M., Hong, W., Unger, F., Chen-Engerer, H.-J., Frosch, M. P., et al. (2019). A vicious cycle of β amyloid-dependent neuronal hyperactivation. *Science* 365, 559–565. doi: 10.1126/science.aay0198

Conflict of Interest: GK is an employee of ISAR bioscience. KB is an employee of Roche. AR has received research support and speaker honoraria from Siemens. MB received speaker honoraria from GE healthcare, Roche, and LMI and is an advisor of LMI.

The remaining authors declare that the research was conducted in the absence of any commercial or financial relationships that could be construed as a potential conflict of interest.

Publisher's Note: All claims expressed in this article are solely those of the authors and do not necessarily represent those of their affiliated organizations, or those of the publisher, the editors and the reviewers. Any product that may be evaluated in this article, or claim that may be made by its manufacturer, is not guaranteed or endorsed by the publisher.

Copyright © 2022 Blume, Deussing, Biechele, Peters, Zott, Schmidt, Franzmeier, Wind, Eckenweber, Sacher, Shi, Ochs, Kleinberger, Xiang, Focke, Lindner, Gildehaus, Beyer, von Ungern-Sternberg, Bartenstein, Baumann, Adelsberger, Rominger, Cumming, Willem, Dorostkar, Herms and Brendel. This is an open-access article distributed under the terms of the Creative Commons Attribution License (CC BY). The use, distribution or reproduction in other forums is permitted, provided the original author(s) and the copyright owner(s) are credited and that the original publication in this journal is cited, in accordance with accepted academic practice. No use, distribution or reproduction is permitted which does not comply with these terms.